

## $B$ Decays and CP Violation from $BABAR$

F. Palombo

Università degli Studi di Milano, Dipartimento di Fisica and INFN, I-20133 Milano, Italy  
*on behalf of the BABAR Collaboration*

### Abstract

We present some recent  $BABAR$  measurements of the magnitudes of the elements  $V_{ub}$  and  $V_{cb}$  of the Cabibbo-Kobayashi-Maskawa quark-mixing matrix, and of the angles  $\alpha$  and  $\gamma$  of the unitary triangle of the standard model of the electroweak interactions. Most of the measurements presented here are based on the full  $BABAR$   $\Upsilon(4S)$  dataset, consisting of about  $467 \times 10^6$   $B\bar{B}$  pairs.

Invited talk presented at the 8<sup>th</sup> Latin American Symposium on High Energy Physics ,  
6/12/2010—12/12/2010, Valparaiso, Chile

# 1 Introduction

The elements of the Cabibbo-Kobayashi-Maskawa (*CKM*) quark-mixing matrix [1] are fundamental parameters of the Standard Model (*SM*) of electroweak interactions. *CKM* matrix is determined by four independent parameters, interpreted as three mixing angles between the three pairs of quark generations and a non-trivial complex phase which in the *SM* represents the only source of Charge-Parity (*CP*) violation.

The unitarity condition of the *CKM* matrix leads to six relations, which represent six triangles in the complex plane. Four of these triangles are degenerate with one side much smaller than the other two and are not useful in the present experimental sensitivity. The remaining two triangles have the lengths of all sides of order  $\lambda^3$ , where  $\lambda$  is the sine of the Cabibbo angle ( $\lambda \sim 0.225$ ). To leading order in  $\lambda$ , these two triangles coincide. The *CKM* Unitary Triangle (*UT*) is taken the one that represents the relation  $V_{ub}^* V_{ud} + V_{cb}^* V_{cd} + V_{tb}^* V_{td} = 0$ . This triangle can be rescaled [2] in order to have one side of unitary length on one axis as shown in Fig. 1:

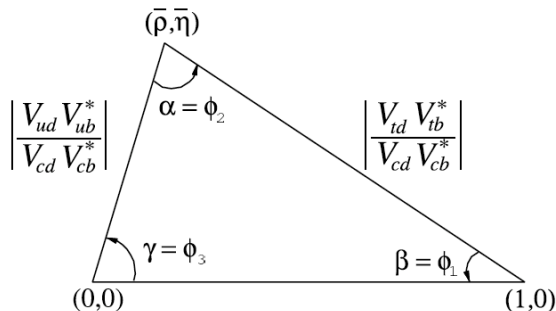


Figure 1: Unitary Triangle

The lengths of the other two sides are :

$$R_u \equiv \left| \frac{V_{ud} V_{ub}^*}{V_{cd} V_{cb}^*} \right| = (1 - \frac{\lambda^2}{2}) \frac{1}{\lambda} \left| \frac{V_{ub}}{V_{cb}} \right|, \quad R_t \equiv \left| \frac{V_{td} V_{tb}^*}{V_{cd} V_{cb}^*} \right| = \frac{1}{\lambda} \left| \frac{V_{tb}}{V_{cb}} \right| \quad (1)$$

while the angles [3] are defined by:

$$\alpha \equiv \arg \left[ -\frac{V_{td} V_{tb}^*}{V_{ud} V_{ub}^*} \right], \quad \beta \equiv \arg \left[ -\frac{V_{cd} V_{cb}^*}{V_{td} V_{tb}^*} \right], \quad \gamma \equiv \arg \left[ -\frac{V_{ud} V_{ub}^*}{V_{cd} V_{cb}^*} \right], \quad (2)$$

In the *B* meson sector there are many independent ways to measure *UT* sides and angles, over-constraining this triangle. To test the *SM* picture of *CP* violation, we have to check that the *UT* is a closed triangle. If experimental measurements of magnitudes of *UT* sides and angles are inconsistent with a closed triangle, we have hints that New Physics (*NP*) beyond the *SM* contributes to *CP* violation.

The *BABAR* [4] and Belle [5] experiments, operating at the PEP-II and KEKB *B*-factories respectively, have provided in the last ten years very precise measurements in the *B* meson sector. The primary goal of these experiments was the verification of the *SM* description of *CP* violation and this goal has been fully reached. The observation of mixing-induced *CP* violation in  $B^0 \rightarrow J/\psi K_S^0$  decays [6], as well as in the charmless penguin-diagram dominated  $B^0 \rightarrow \eta' K^0$  decays [7, 8], and of

direct  $CP$  violation both in  $B^0 \rightarrow \pi^+\pi^-$  and in  $B^0 \rightarrow K^+\pi^-$  decays [9], are all in agreement with  $SM$  predictions.

The  $UT$  angle  $\beta$  has been measured with high precision from time-dependent  $CP$  asymmetries in neutral  $B$  meson decays to  $CP$  eigenstates containing a charmonium and a  $K^{(*)0}$  [8, 10] and will not be covered in this presentation.

In the following, we present some recent  $BABAR$  measurements of the magnitudes of  $CKM$  elements  $V_{ub}$  and  $V_{cb}$ , and of the  $UT$  angles  $\alpha$  and  $\gamma$ .

## 2 Unitary Triangle Sides

The measurement of  $|V_{ub}|$  and  $|V_{cb}|$  has a crucial role in the test of the  $SM$ . In fact, as shown in Fig. 1 and in Eq. 1, the ratio  $\frac{|V_{ub}|}{|V_{cb}|}$  is proportional to the length of  $UT$  side that is opposite to the precisely measured angle  $\beta$ . The value of this ratio constraints the upper vertex of the  $UT$ .  $|V_{ub}|$  and  $|V_{cb}|$  appear in the differential decay rate of semileptonic  $B$  decays to charmless and charm final states, respectively. Differently from hadronic  $B$  decays, in such semileptonic  $B$  decays hadronic and leptonic currents of the amplitude factorize.

Both  $|V_{ub}|$  and  $|V_{cb}|$  can be measured with an exclusive approach where the final state hadron is exclusively reconstructed and with an inclusive approach where all hadronic final states are summed. In these two approaches the hadronic current, difficult to evaluate, relies on different QCD calculations.

### 2.1 Inclusive Measurement of $|V_{ub}|$

The magnitude of  $V_{ub}$  can be determined from inclusive semileptonic  $\bar{B}$  decays to charmless final states  $X_u l \bar{\nu}$ , where  $l = e$  or  $\mu$ , and  $X_u$  is a hadronic system (without charm). The real difficulty in this inclusive measurement comes from the overwhelming charm background from  $\bar{B} \rightarrow X_c l \bar{\nu}$  which has a rate fifty times larger and an event topology very similar to signal.

In a recent analysis [11]  $BABAR$ , using the full dataset of  $467 \times 10^6$   $B\bar{B}$  pairs, has measured Partial Branching Fractions (PBF), restricting the analysis in selected regions of the phase space where most effective is the suppression of the charm background. The event selection uses a hadronic tag: in the sample of  $\Upsilon(4S) \rightarrow B\bar{B}$  one  $B$  decaying into hadrons is fully reconstructed ( $B_{tag}$ ) while the other  $B$  ( $B_{recoil}$ ) is identified by the presence of an electron or muon. The  $B_{tag}$  is reconstructed in many exclusive hadronic decays  $B_{tag} \rightarrow \bar{D}^* Y^\pm$ , where the hadronic system  $Y^\pm$  consists of hadrons and has a total charge of  $\pm 1$ . More than 1000 hadronic decay modes are reconstructed.

In the  $B_{recoil}$  rest-frame we require one lepton with momentum  $p_l^* > 1$  GeV/ $c$  and the hadronic system  $X$  is reconstructed from charged particles and neutral clusters not associated to the  $B_{tag}$  or the charged lepton. Neutrino is reconstructed from missing four-momentum in the whole event. Requirements on several kinematic observables were applied in different phase space regions to select the final signal events.

PBFs are measured in several regions of phase space and are normalized to the total semileptonic branching fraction, thus reducing several systematic uncertainties. Considering the most inclusive measurement (based only on the requirement  $p^* > 1.0$  GeV/ $c$ ), from a two-dimensional fit to the hadronic invariant mass and to the leptonic invariant mass squared we measure :

$$\Delta\mathcal{B}(\bar{B} \rightarrow X_u l \bar{\nu}; p_l^* > 1.0 \text{ GeV}/c) = (1.80 \pm 0.13 \pm 0.15) \times 10^{-3} \quad (3)$$

where the first uncertainty is statistical and the second systematic.

To translate the PBFs measurements into  $|V_{ub}|$  we need a theoretical extrapolation to the full space space, including perturbative and non perturbative QCD effects. This extrapolation has been done using four different models from Bosch, Lange, Neubert, and Paz (BLNP) [12], Gambino, Giordano, Ossola, and Uraltsev (GGOU) [13], Andersen and Gardi (DGE) [14], and Aglietti, Di Lodovico, Ferrera, and Ricciardi (ADFR) [15]. Making an arithmetic mean average of these four calculations, we obtain the result:

$$|V_{ub}| = (4.31 \pm 0.35) \times 10^{-3} \quad (4)$$

This result with a total uncertainty of about 8% is comparable with Belle result [16].

## 2.2 Exclusive Measurement of $|V_{ub}|$ from $B \rightarrow (\pi, \rho)l\nu$ Decays

*BABAR* has measured  $|V_{ub}|$  also with an exclusive approach in the charmless semileptonic decays  $B \rightarrow \pi l\nu$  and  $B \rightarrow \rho l\nu$  [17]. This analysis is based on a data sample of  $377 \times 10^6$   $B\bar{B}$  pair. In this exclusive analysis compared to the corresponding inclusive one we have a better control of the background but lower signal yields. The differential decay rate to the final state containing the pseudoscalar meson  $\pi$  can be written in the form:

$$\frac{d\Gamma(B^0 \rightarrow \pi^- l^+ \nu)}{dq^2 d\cos\theta_{Wl}} = |V_{ub}|^2 \frac{G_F^2 p_\pi^3}{32\pi^3} \sin^2\theta_{Wl} |f_+(q^2)|^2, \quad (5)$$

where  $G_F$  is the Fermi coupling constant,  $p_\pi$  is the momentum of the pion in the rest frame of the  $B$  meson,  $q^2$  is the momentum transfer squared from the  $B$  meson to the final-state hadron (mass squared of the virtual  $W$ ),  $\theta_{Wl}$  is the angle of the charged-lepton momentum in the  $W$  rest frame with respect to the direction of the  $W$  boost from the  $B$  rest frame, and  $f_+(q^2)$  is the form factor parameterizing the hadronic matrix element.

For the decays with the vector-meson  $\rho$  in the final state the hadron matrix element is parameterized in terms of three form factors [17].

The four charmless semileptonic decays  $B^0 \rightarrow \pi^- l^+ \nu$ ,  $B^+ \rightarrow \pi^0 l^+ \nu$ ,  $B^0 \rightarrow \rho^- l^+ \nu$ , and  $B^+ \rightarrow \rho^0 l^+ \nu$  are reconstructed, requiring a high-momentum lepton ( $l = e, \mu$ ), a hadron ( $\pi, \rho$ ), and a neutrino. The neutrino is reconstructed from the missing energy and momentum in the event. All tracks and neutral clusters not associated to the signal must be consistent with a  $B$  decay. There are three types of background: continuum,  $B\bar{B}$  and other  $B \rightarrow X_u l\nu$  decay modes.  $B\bar{B}$  is the largest source of background, in particular charmed semileptonic  $B \rightarrow X_c l\nu$ . Furthermore the isolation of the individual exclusive charmless decays from all the other  $B \rightarrow X_u l\nu$  is difficult (they represent only 10% of the total). The three types of background are suppressed using a neural network based on seven discriminating variables [17].

Branching fractions are extracted from extended binned maximum likelihood fit to  $m_{ES}$ ,  $\Delta E$ , and  $q^2$ .  $m_{ES}$  is the beam-energy substituted  $B$  mass and  $\Delta E$  is the difference between the reconstructed and expected energy of the  $B$  candidate. The four channels ( $\pi^-$ ,  $\pi^0$ ,  $\rho^-$ , and  $\rho^0$ ) are fitted simultaneously imposing isospin constraint. Branching fraction results from this fit are:

$$\begin{aligned} \mathcal{B}(B^0 \rightarrow \pi^- l^+ \nu) &= (1.41 \pm 0.05 \pm 0.07) \times 10^{-4} \\ \mathcal{B}(B^0 \rightarrow \rho^- l^+ \nu) &= (1.75 \pm 0.15 \pm 0.27) \times 10^{-4}, \end{aligned} \quad (6)$$

where the first uncertainty is statistical and the second systematic.

To extract  $|V_{ub}|$  using Eq. 5 we need theoretical input for the form factor. For the  $B \rightarrow \pi l \nu$  partial differential decay rates  $\Delta\mathcal{B}$  are measured in six bins of  $q^2$  and results are compared (see Fig. 2) with calculations of quark-model (ISGW2) [18], QCD light-cone sum rules (LCSR1) [19], (LCSR2) [20], and unquenched lattice QCD calculations (HPQCD) [21]. The shape of the form factor is obtained directly from the data.

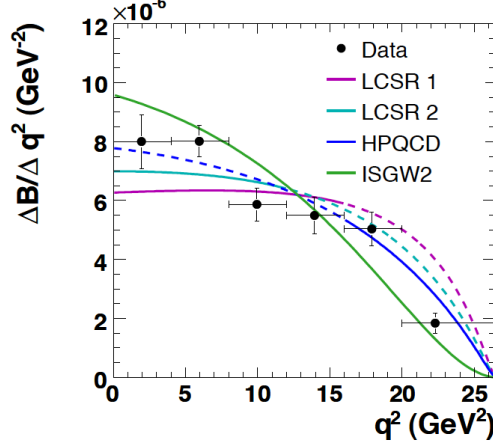


Figure 2: Shape comparisons of measured partial branching fractions of  $B^0 \rightarrow \pi^- l^+ \nu$  to various form factor theoretical predictions which have been normalized to the measured total branching fraction. The dashed line represents the extrapolations of QCD predictions to the full  $q^2$  range.

The magnitude of  $V_{ub}$  is extracted with two methods. In the first one  $|V_{ub}|$  is obtained by integration of form factor prediction over the relevant  $q^2$  interval using the relations:

$$|V_{ub}| = \sqrt{\frac{\Delta\mathcal{B}(q_{min}^2, q_{max}^2)}{\tau_0 \Delta\zeta(q_{min}^2, q_{max}^2)}}, \quad \Delta\zeta(q_{min}^2, q_{max}^2) = \frac{G_F^2}{24\pi^3} \int_{q_{min}^2}^{q_{max}^2} p_\pi^3 |f_+(q^2)|^2 dq^2,$$

where  $\tau_0 = 1.530 \pm 0.009$  is the  $B^0$  lifetime [22].

In Table 1 we show (first three rows) the extracted values of  $|V_{ub}|$ . First quoted uncertainty is experimental and the second theoretical from the form-factor integral  $\Delta\zeta$ .

Table 1:  $|V_{ub}|$  extracted from  $B \rightarrow \pi l \nu$  in various  $q^2$  intervals and form factor calculations. In the last row  $|V_{ub}|$  measured in the simultaneous fit of *BABAR* data to recent lattice calculations.

	$q^2$ Range ( $GeV^2$ )	$\Delta\mathcal{B}$ ( $10^{-4}$ )	$\Delta\zeta$ ( $ps^{-1}$ )	$ V_{ub} $ ( $10^{-3}$ )
LCSR 1	0 – 16	$1.10 \pm 0.07$	$5.44 \pm 1.43$	$3.63 \pm 0.12^{+0.59}_{-0.40}$
LCSR 2	0 – 12	$0.88 \pm 0.06$	$4.00^{+1.01}_{-0.95}$	$3.78 \pm 0.13^{+0.55}_{-0.40}$
HPQCD	16 – 26.4	$0.32 \pm 0.03$	$2.02 \pm 0.55$	$3.21 \pm 0.17^{+0.55}_{-0.36}$
FNAL/MILC	0 – 26.4	$1.41 \pm 0.09$	–	$2.95 \pm 0.31$

In the second method we do a simultaneous fit to the most recent lattice calculations and *BABAR* data using the linear or quadratic BGL parameterization for the full  $q^2$  range [23]. In Fig. 3 we show results of such a fit. The solid line represents the quadratic (3 parameters + 1 normalization) BGL fit while the shaded region shows the uncertainty of the fitted function. The value of  $|V_{ub}|$  extracted in this method using the normalization predicted by FNAL/MILC Collaboration [24] is also shown (last row) in Table 1. The quoted total uncertainty of 10% is dominated by the theory uncertainty of 8.5%.

If we compare the *BABAR* exclusive and inclusive  $|V_{ub}|$  determinations, we see a discrepancy at the level of about  $2.7\sigma$ . A similar discrepancy at the level of about  $2.3\sigma$  is also present in Belle results.

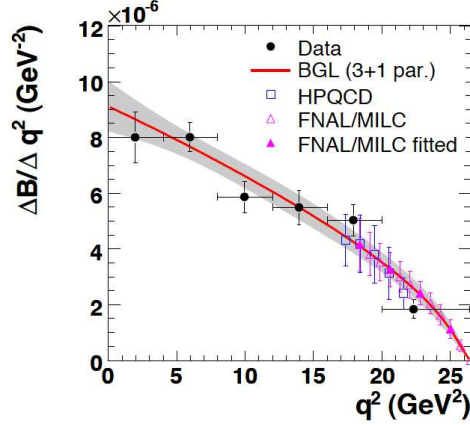


Figure 3: Simultaneous fit of quadratic BGL parameterization to data. The shaded band indicates the uncertainty of the fitted function.

### 2.3 $|V_{ub}|$ and the Leptonic $B^+ \rightarrow \tau^+ \nu_\tau$ Decay

The purely leptonic  $B$  decay to  $\tau \nu_\tau$  proceeds in  $SM$  through  $W$  boson annihilation with a branching fraction:

$$\mathcal{B}(B^+ \rightarrow \tau^+ \nu_\tau) = f_B^2 |V_{ub}|^2 \frac{G_F^2 m_B m_\tau^2}{8\pi} \left[ 1 - \frac{m_\tau^2}{m_B^2} \right]^2 \tau_{B^+}$$

The  $SM$  estimate for this branching fraction is of the order of  $10^{-4}$ . However contributions from  $NP$  scenarios [25] may enhance this expectation.

*BABAR* has studied this decay mode both with a semileptonic tagging method [26] and with a hadronic tag method [27]. We present here results of the analysis based on hadronic tag. The  $B_{tag}$  candidates are reconstructed from  $B^- \rightarrow M^0 X^-$ , where  $M^0$  denotes a  $D^{(*)0}$  or  $J/\psi$ , and  $X^-$  is a hadronic system with total charge -1. The signal  $B$  candidate is reconstructed considering the most abundant decays  $\tau^+ \rightarrow e^+ \nu \bar{\nu}$ ,  $\tau^+ \rightarrow \mu^+ \nu \bar{\nu}$ ,  $\tau^+ \rightarrow \pi^+ \nu$ , and  $\tau^+ \rightarrow \rho^+ \nu$ . The most discriminating variable in this analysis is  $E_{extra}$ , sum of the energies of neutral clusters not associated with the  $B_{tag}$  (or with the  $\pi^0$  from the  $\tau^+ \rightarrow \rho^+ \nu$ ). Signal yield is extracted from an extended unbinned maximum likelihood fit to all four  $\tau$  decay modes. Table 2 summarizes fit results.

Table 2: Reconstruction efficiency  $\epsilon$ , branching fraction and significance (only statistical uncertainty) from the fit to the four decay modes separately and constrained to the same branching fraction.

Decay Mode	$\epsilon \times 10^{-4}$	Branching Fraction ( $\times 10^{-4}$ )	Significance ( $\sigma$ )
$\tau^+ \rightarrow e^+ \nu \bar{\nu}$	2.73	$0.39^{+0.89}_{-0.79}$	0.5
$\tau^+ \rightarrow \mu^+ \nu \bar{\nu}$	2.92	$1.23^{+0.89}_{-0.80}$	1.6
$\tau^+ \rightarrow \pi^+ \nu$	1.55	$4.0^{+1.5}_{-1.3}$	3.3
$\tau^+ \rightarrow \rho^+ \nu$	0.85	$4.3^{+2.2}_{-1.9}$	2.6
Combined	8.05	$1.80^{+0.57}_{-0.54}$	3.6

Including systematic uncertainties the branching fraction is  $\mathcal{B}(B^+ \rightarrow \tau^+ \nu_\tau) = (1.80^{+0.57}_{-0.54} \pm 0.26) \times 10^{-4}$ . The null hypothesis ( $\mathcal{B}(B^+ \rightarrow \tau^+ \nu_\tau) = 0$ ) is excluded with a significance (including systematic uncertainty) at the level of  $3.3 \sigma$ .

Combining this result and the other *BABAR* measurement using a semileptonic tag and a statistical independent sample [26], we obtain the result  $\mathcal{B}(B^+ \rightarrow \tau^+ \nu_\tau) = (1.76 \pm 0.49) \times 10^{-4}$ , where the uncertainty includes both statistical and systematic uncertainties.

Results are consistent with the corresponding Belle analyses using hadronic tag [28] and semileptonic tag [29].

In a global fit excluding the branching fraction of  $B^+ \rightarrow \tau^+ \nu_\tau$ , UTfit [30] finds for this branching fraction a value of  $(0.79 \pm 0.07) \times 10^{-4}$  while CKMfitter [31] finds  $(0.786^{+0.179}_{-0.083}) \times 10^{-4}$ . These expectations (see Fig. 4) are about  $2.5\sigma$  lower than the experimental result.

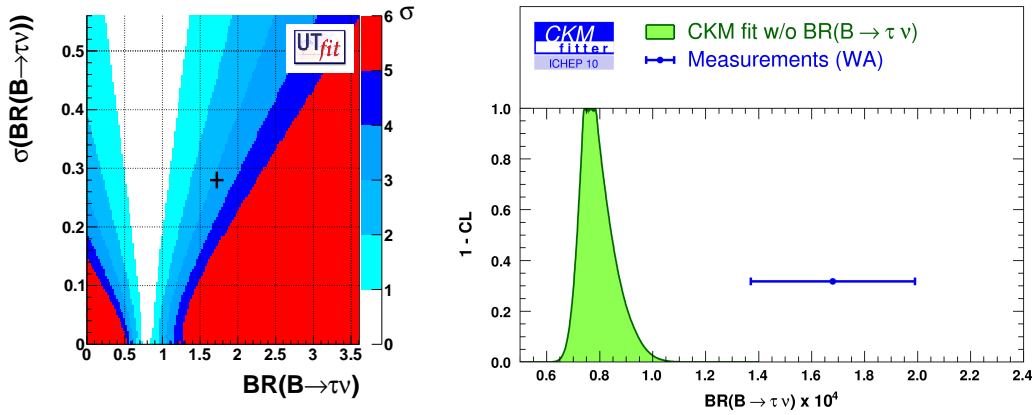


Figure 4: Branching fraction of the decay  $B^+ \rightarrow \tau^+ \nu_\tau$  as predicted from a global fit by UTfit (on the left) and by CKMfitter (on the right) compared to the experimental measurement.

## 2.4 Exclusive Measurement of $|V_{cb}|$ in $\bar{B} \rightarrow D l^- \bar{\nu}_l$ Decays

$|V_{cb}|$  has been measured both in inclusive semileptonic  $B$  decays [32] and in exclusive decays  $\bar{B} \rightarrow D l^- \bar{\nu}_l$  and  $\bar{B} \rightarrow D^* l^- \bar{\nu}_l$  [33] with  $l = e$  or  $\mu$ . We present here a recent *BABAR* measurement of

$|V_{cb}|$  from the differential decay rate of exclusive decays  $\bar{B} \rightarrow Dl^- \bar{\nu}_l$  [34] :

$$\frac{d\Gamma(\bar{B} \rightarrow Dl\bar{\nu}_l)}{dw} = \frac{G_F^2}{48\pi^3\hbar} m_D^3 (m_B + m_D)^2 (w^2 - 1)^{\frac{3}{2}} |V_{cb}|^2 \mathcal{G}(w) \quad (7)$$

where  $m_B$  and  $m_D$  are the masses of  $B$  and  $D$  mesons, respectively. The variable  $w$  is the product of the  $B$  and  $D$  meson four-velocities,  $w = (m_B^2 + m_D^2 - q^2)/(2m_B m_D)$ , where  $q^2 \equiv (p_B - p_D)^2$ , and  $p_B$  and  $p_D$  are the four-momenta of the  $B$  and  $D$  mesons.  $\mathcal{G}(w)$  is the form factor which is normalized to unity at zero recoil in heavy quark mass limit [35].

$|V_{cb}|$  is determined by extrapolating the differential decay rate to  $w = 1$ . In this extrapolation the shape of the form factor is needed. In this analysis the parameterization proposed in Ref. [36] has been adopted. Corrections to heavy quark limit have been calculated with unquenched [37] and quenched [38] lattice QCD.

Semileptonic signal  $B$  events are searched for the recoil of fully reconstructed hadronic  $B$  mesons ( $B_{tag}$ ). They are identified by their missing mass squared, calculated from the measured four-momenta of the particles in the event,  $m_{miss}^2 = [p_{\Upsilon(4S)} - p_{B_{tag}} - p_D - p_l]^2$ . This variable peaks at zero for signal events. Signal yields are obtained from least-squares fit to the missing mass squared spectrum in ten equal-size intervals of  $w$  in the interval  $1 < w < 1.6$ . First fits are done separately on the neutral and charged  $\bar{B} \rightarrow Dl^- \bar{\nu}_l$  samples and then on the combined sample. We show in Fig. 5 the measured  $m_{miss}^2$  distributions and fit results (sum of the solid histograms) for two different  $w$  intervals.

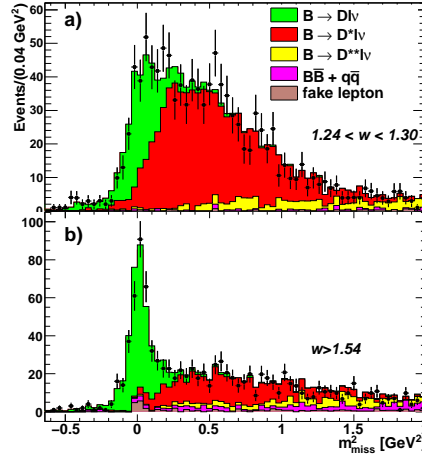


Figure 5:  $m_{miss}^2$  distributions in two different  $w$  intervals and fit results for  $B^- \rightarrow D^0 l^- \bar{\nu}$

We obtain  $\mathcal{G}(1)|V_{cb}|$  and the form-factor slope  $\rho^2$  from a least-squares fit to the  $w$  distribution. We show in Fig. 6 data and fit results on the combined signal yields of  $B^- \rightarrow D^0 l^- \bar{\nu}_l$  and  $\bar{B}^0 \rightarrow D^+ l^- \bar{\nu}_l$ . The measured  $\mathcal{G}(1)|V_{cb}|$ , form-factor slope  $\rho^2$  and branching fraction obtained from the fit to the combined  $\bar{B}^0/B^-$  sample are:

$$\begin{aligned} \mathcal{G}(1)|V_{cb}| &= (42.3 \pm 1.9 \pm 1.4) \times 10^{-3} \\ \rho^2 &= 1.20 \pm 0.09 \pm 0.04 \\ \mathcal{B}(\bar{B} \rightarrow Dl^- \bar{\nu}_l) &= (2.15 \pm 0.06 \pm 0.09)\% \end{aligned} \quad (8)$$



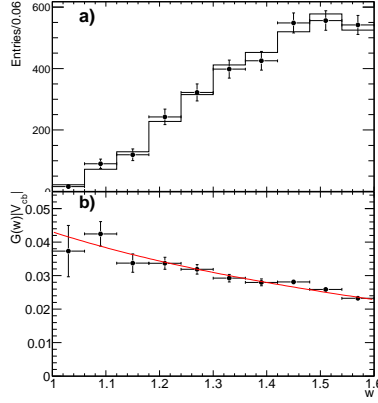


Figure 6: (a)  $w$  distribution of the signal yield of the combined sample. Data points are compared to the overall fit results (histogram); (b)  $\mathcal{G}(w)|V_{cb}|$  distribution corrected for the reconstruction efficiency with the fit superimposed.

The extracted value of  $|V_{cb}|$ , applying an unquenched lattice calculation [37], is:

$$|V_{cb}| = (39.2 \pm 1.8 \pm 1.3 \pm 0.9) \times 10^{-3}, \quad (9)$$

where the uncertainties are statistical, systematic and theoretical (in  $\mathcal{G}(1)$ ), respectively. As for  $|V_{ub}|$ ,  $|V_{cb}|$  inclusive results tend to be higher than the exclusive results [39].

### 3 Unitary Triangle Angle $\alpha$

$B^0$  decays to  $\pi^+\pi^-$ ,  $\rho^\pm\pi^\mp$ ,  $\rho^+\rho^-$ , and  $a_1(1260)^\pm\pi^\mp$  proceed dominantly through the  $\bar{b} \rightarrow \bar{u}u\bar{d}$  process and have been used to measure the time-dependent  $CP$  asymmetries and extract the angle  $\alpha$ . In all these  $B$  decay modes the presence of sizeable loop (penguin) contributions introduces a distortion (penguin pollution) in the measurement of  $\alpha$ . Instead of  $\alpha$  one measures  $\alpha_{eff}$ . To take into account this distortion several approaches have been proposed: isospin symmetry [42], time-dependent Dalitz plot analysis [43], or approximate  $SU(3)$  flavor symmetry [44].

We present here a recent *BABAR* update of the measurement of angle  $\alpha$  in the decay modes  $B \rightarrow \rho\rho$  and the first extraction of this angle from the decay modes  $B^0 \rightarrow a_1(1260)^\pm\pi^\mp$ .

#### 3.1 Angle $\alpha$ from $B \rightarrow \rho\rho$ Decays

In the  $B \rightarrow \rho\rho$  decay modes the correction  $\Delta\alpha = \alpha - \alpha_{eff}$  has been obtained with an isospin analysis involving the  $B \rightarrow \rho^+\rho^-$ ,  $\rho^0\rho^0$ , and  $\rho^+\rho^0$  decays. In a recent analysis [45] *BABAR* has updated with the full dataset the measurement of the branching fraction and longitudinal polarization fraction  $f_L$  in the  $B \rightarrow \rho^+\rho^0$  decay, obtaining:

$$\begin{aligned} \mathcal{B}(B^+ \rightarrow \rho^+\rho^0) &= (23.7 \pm 1.4 \pm 1.4) \times 10^{-6} \\ f_L &= (0.950 \pm 0.015 \pm 0.006) \end{aligned} \quad (10)$$

These measured values of  $\mathcal{B}(B^+ \rightarrow \rho^+ \rho^0)$  and  $f_L$  are higher than those of the previous *BABAR* analysis [46] and this has an important effect in the isospin analysis.  $\mathcal{B}(B^+ \rightarrow \rho^+ \rho^0)$  represents in fact the common base of the two isospin triangles of the  $B$  and the  $\bar{B}$  decays. The large value of  $\mathcal{B}(B^+ \rightarrow \rho^+ \rho^0)$  flattens the two isospin triangles.

An isospin analysis has been performed using the new branching fraction and  $f_L$  values for the  $B \rightarrow \rho^+ \rho^0$  decay together with previous results for  $B^0 \rightarrow \rho^+ \rho^-$  [47], and for  $B^0 \rightarrow \rho^0 \rho^0$  [48]. The four possible solutions of  $\Delta\alpha$  are now nearly degenerate while the eight-fold ambiguity on  $\alpha$  degenerates into a four-fold ambiguity with peaks near  $0^\circ$ ,  $90^\circ$  (two degenerate peaks), and  $180^\circ$ . We take the solution for  $\alpha$  near  $90^\circ$  which is consistent with the global CKM fits [30, 31]. Projections of the 1-CL scan on  $\alpha$  and  $\Delta\alpha$  are shown in Fig. 7.

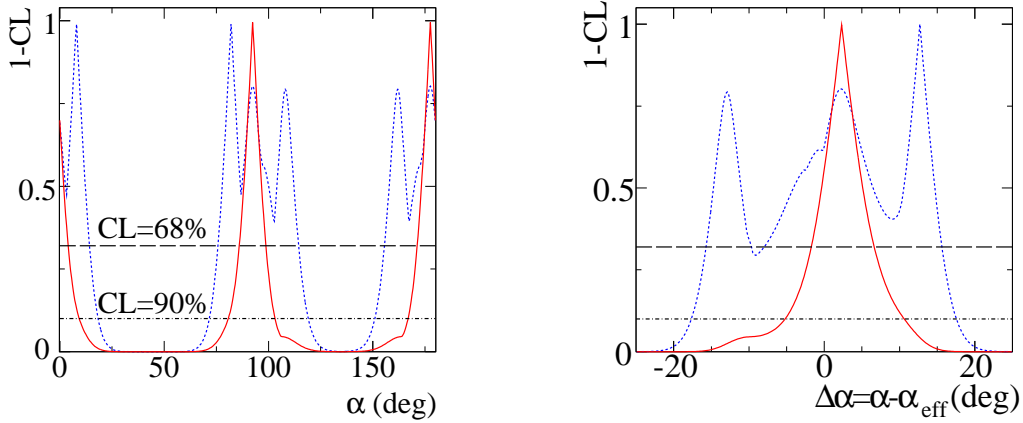


Figure 7: Projections of 1-CL scan on  $\alpha$  and  $\Delta\alpha$ . The solid (dotted) curves show the results using the branching fraction  $\mathcal{B}(B^+ \rightarrow \rho^+ \rho^0)$  measured in this analysis (prior to this analysis). See supplemental material in Ref. [45].

The solution for  $\alpha$  and  $\Delta\alpha$  at 68% CL are  $\alpha = (92.4^{+6.0}_{-6.5})^\circ$  and  $-1.8^\circ < \Delta\alpha < 6.7^\circ$ . These results are significantly improved compared to those of the previous *BABAR* analysis. This measurement is currently the most precise single measurement of  $\alpha$ .

### 3.2 Angle $\alpha$ from $B \rightarrow a_1(1260)\pi$ Decays

The final states in the  $B^0(\bar{B}^0) \rightarrow a_1^\pm \pi^\mp$  [49] decays are not  $CP$  eigenstates. So to extract  $\alpha$  from these channels one has to consider simultaneously  $B^0(\bar{B}^0) \rightarrow a_1^+ \pi^-$  and  $B^0(\bar{B}^0) \rightarrow a_1^- \pi^+$  [50]. *BABAR* has observed these decay modes [51] and measured the time-dependent  $CP$  asymmetries and  $\alpha_{eff}$  [52]. In these decay modes full isospin analysis or time-dependent Dalits plot approach to correct for the distortion  $\Delta\alpha$  are not viable due to the limited statistics of available data samples, difficulties because of the four particles in the final states, and uncertainties in the  $a_1$  meson parameters and lineshape.

Applying flavor  $SU(3)$  symmetry [53] one can determine an upper bound on  $\Delta\alpha = |\alpha - \alpha_{eff}|$  by relating the  $B^0 \rightarrow a_1^\pm \pi^\mp$  decay rates with those of the  $\Delta S = 1$  transitions involving the same  $SU(3)$  multiplet of  $a_1$ ,  $B \rightarrow a_1 K$  and  $B \rightarrow K_{1A} \pi$ . Branching fractions of  $B \rightarrow a_1 K$  have been already measured by *BABAR* [54]. The  $K_{1A}$  meson is a nearly equal admixture of  $K_1(1270)$  and

$K_1(1400)$  resonances [55]. The rates of  $B \rightarrow K_{1A}\pi$  decays can be derived from the decay rates of  $B \rightarrow K_1(1270)\pi$  and  $B \rightarrow K_1(1400)\pi$ .

The  $K_1(1270)$  and  $K_1(1400)$  axial vector mesons are broad resonances with nearly equal masses. Both mesons decay to the same final state  $K\pi\pi$ , although through different intermediate states. However, since the intermediate decays proceed almost at threshold, the available phase spaces overlap and interference effects can be sizeable. The strategy of a recent *BABAR* analysis [56] relies on the reconstructed  $K\pi\pi$  invariant mass spectrum in the [1.1, 1.8] GeV range to distinguish between  $K_1(1270)$  and  $K_1(1400)$ , including interference effects in the signal model. A two-resonance, six-channel  $K$ -matrix model [57] in the P-vector approach [58] is used to describe the resonant  $K\pi\pi$  system for the signal.

A MC technique is used to estimate a probability region for the bound on  $|\Delta\alpha|$  and the result is  $|\Delta\alpha| < 11^\circ(13^\circ)$  at 68% (90%) probability [56]. Combining this bound on  $\Delta\alpha$  and the measured  $\alpha_{eff}$  [52], we have  $\alpha = (79 \pm 7 \pm 11)^\circ$ , where the first uncertainty is statistical and systematic combined and the second uncertainty is due to penguin pollution.

## 4 Unitary Triangle Angle $\gamma$

The angle  $\gamma$  is the only  $CP$ -violating parameters that can be cleanly determined using solely tree-level  $B$  decays. In absence of penguin contribution, it is almost largely unaffected by the presence of  $NP$ . We can access this angle in the interference between the color-favored decay  $B^- \rightarrow D^{(*)0}K^{(*)-}$  ( $b \rightarrow c\bar{u}s$  transition) and the color and CKM suppressed process  $B^- \rightarrow \bar{D}^{(*)0}K^{(*)-}$  ( $b \rightarrow u\bar{c}s$  transition). Here  $D$  refers to any admixture of  $D^0$  and its  $CP$ -conjugate  $\bar{D}^0$ . The two interfering amplitudes differ by a factor  $r_B e^{i(\delta_B \pm \gamma)}$  where  $r_B$  is the magnitude of the ratio of the two amplitudes, and  $\delta_B$  is their relative strong phase.

Because of the limited available data sample and the small branching fractions of the target  $B$  decay modes, angle  $\gamma$  is the most difficult to measure and the less precisely known UT angle.

Several time-integrated methods have been proposed to exploit this interference and extract angle  $\gamma$ . The most productive today are: the Gronau, London, Wiler (GLW) method [59] where the Cabibbo-suppressed  $D$  decays to  $CP$ -eigenstates (such as  $K^+K^-$  or  $K_S^0\pi^0$ ); the Atwood, Duni-etz, Soni (ADS) method [60] where  $D$  is reconstructed in Cabibbo-favored and double Cabibbo-suppressed final states (such as  $K^\pm\pi^\mp$ ); the Giri, Grossman, Soffer, Zupan (GGSZ) method where the  $D$  meson decays to three-body self-conjugate final states (such as  $K_S^0\pi^+\pi^-$  or  $K_S^0K^+K^-$ ) which are analyzed on a Dalitz plot. *BABAR* recently updated  $\gamma$  measurements with the GLW method [62], with the ADS method [63], and GGSZ method [64]. We present here only the results obtained with the GGSZ method.

### 4.1 Angle $\gamma$ Measured in a Dalitz Plot Analysis (GGSZ Method)

In a recent analysis based on the full *BABAR* dataset [64] the angle  $\gamma$  has been measured following the GGSZ method. In this analysis the following  $B$  decay modes are reconstructed:  $B^\pm \rightarrow DK^\pm$ ,  $B^\pm \rightarrow D^*K^\pm$  ( $D^* \rightarrow D\pi^0, D\gamma$ ) and  $B^\pm \rightarrow DK^{*\pm}$  ( $K^{*\pm} \rightarrow K_S^0\pi^\mp$ ) with  $D \rightarrow K_S^0 h^+ h^-$  ( $h = \pi, K$ ).

The three-body  $D$  decays are studied on a Dalitz plot. A simultaneous extended unbinned maximum likelihood fit is done to all the abovementioned  $B$  decay modes, extracting signal and background yields together with the  $CP$ -violating parameters  $x_\mp \equiv r_B \cos(\delta_B \pm \gamma)$  and  $y_\mp \equiv r_B \sin(\delta_B \pm \gamma)$  for  $DK$ ,  $D^*K$ , and  $DK^*$  final states. Using all the measured observables 1-dimensional confidence intervals are constructed following a frequentist approach.

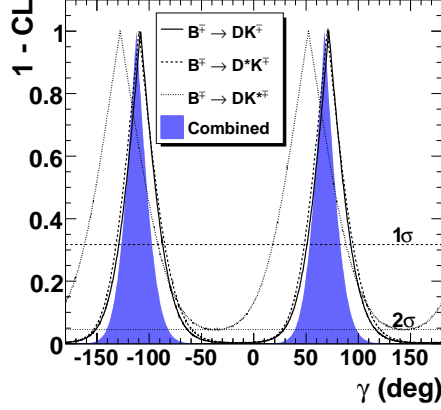


Figure 8: 1-CL scan as a function of  $\gamma$  for  $B^\pm \rightarrow DK^\pm$ ,  $D^*K^\pm$ , and  $DK^{*\pm}$  decays separately, and combined. The dashed (upper) and dotted (lower) horizontal lines correspond to the one- and two-standard deviation intervals, respectively.

In Fig. 8 we show 1-CL as a function of  $\gamma$  for the three B decay channels separately and their combination, including statistical and systematic uncertainties. There is a single ambiguity in the weak and strong phases.

The one- and two-standard deviation intervals for  $\gamma$  and for the three pairs of values  $(r_B, \delta_B)$ ,  $(r_B^*, \delta_B^*)$ , and  $(\kappa r_s, \delta_s)$  for the  $DK$ ,  $D^*K$  and  $DK^*$  respectively, are shown in Tab. 3. The factor  $\kappa = 0.9 \pm 0.1$  in the result for the decay  $B^\pm \rightarrow DK^{*\pm}$  takes into account the  $K^*$  finite width.

Table 3: The one- and two-standard deviation intervals for all relevant parameters. The first uncertainty is statistical. The second and third uncertainties inside  $\{ \}$  brackets are the symmetric uncertainty contributions to the total uncertainty from the experimental and neutral  $D$  decay amplitudes uncertainties.

Parameter	68.3% CL	95.4% CL
$\gamma$ ( $^\circ$ )	$68^{+15}_{-14} \{4, 3\}$	$[39, 98]$
$r_B$ (%)	$9.6 \pm 2.9 \{0.5, 0.4\}$	$[3.7, 15.5]$
$r_B^*$ (%)	$13.3^{+4.2}_{-3.9} \{1.3, 0.3\}$	$[4.9, 21.5]$
$\kappa r_s$ (%)	$14.9^{+6.6}_{-6.2} \{2.6, 0.6\}$	$< 28.0$
$\delta_B$ ( $^\circ$ )	$119^{+19}_{-20} \{3, 3\}$	$[75, 157]$
$\delta_B^*$ ( $^\circ$ )	$-82 \pm 21 \{5, 3\}$	$[-124, -38]$
$\delta_s$ ( $^\circ$ )	$111 \pm 32 \{11, 3\}$	$[42, 178]$

The extracted central value of  $\gamma$  is  $(68 \pm 14 \pm 4 \pm 3)^\circ$  (modulo  $180^\circ$ ). It is inconsistent with no direct  $CP$  violation ( $\gamma = 0$ ) with a significance of  $3.5 \sigma$ . Results of this analysis are consistent with previous *BABAR* results [65] and with those of the Belle Collaboration [66].

## 5 Summary and Conclusions

We have presented results of some recent *BABAR* measurements of the magnitudes of the CKM matrix elements  $V_{ub}$  and  $V_{cb}$ , and of the UT angles  $\alpha$  and  $\gamma$ . In these analyses *BABAR* using final dataset significantly decreased the uncertainties on the measurements of  $|V_{ub}|$  and  $|V_{cb}|$ , thanks to the increased dimension of the data sample, improved experimental techniques and theoretical inputs.

A discrepancy at the level of about  $2.7\sigma$  is present between exclusive and inclusive  $|V_{ub}|$  determinations. Similar discrepancy is also present in the results of the Belle analyses.  $|V_{cb}|$  inclusive results, as for  $V_{ub}$ , tend to be higher than the exclusive results. The inclusive and exclusive approaches however have different theoretical input: in the inclusive approach parton level calculations need perturbative corrections and non perturbative extrapolations while the exclusive approach is based on the present lattice QCD and light cone sum rules understanding of form factors. It is not clear the source of these discrepancies which may be due to some not well calibrated tool or be the effect of unattributed uncertainties.

The updated measurement of the angle  $\alpha$  in the  $B \rightarrow \rho\rho$  is significantly improved with respect to previous *BABAR* and Belle results. We have also presented a novel measurement of the angle  $\alpha$  in  $B \rightarrow a_1(1260)\pi$  decays.

Finally we have reported on a recent  $\gamma$  measurement in  $B$  to  $D^{(*)}K$  and  $DK^{*\pm}$  decays using the GGSZ method. This measurement, as well as all other  $\gamma$  measurements at the  $B$ -factories, is statistically limited. A precise  $\gamma$  measurement is an important goal of next generation experiments on flavor physics.

All the presented analyses, based on full or almost full *BABAR* dataset, can be considered final. Results of these analyses as well as all *BABAR* results are essentially in agreement with the expectations of the *SM*. Both *BABAR* and Belle experiments have found no clear effect which can be attributed to *NP*. The limited disagreement with *SM* found in a few cases may be explained either with improved calculations within the *SM* or with *NP* contributions. We need much more precise measurements to improve our sensitivity to *SM* deviations and to *NP* effects. We expect a significant impact on flavor physics from LHCb experiment [67] and from the super flavor factories (superKEKB [68] and SuperB [69]).

## References

- [1] N. Cabibbo, Phys. Rev. Lett. **10**, 531 (1963); M. Kobayashi and T. Maskawa, Prog. Theor. Phys. **49**, 652 (1973).
- [2] The CKM and the Unitary Triangle, Proceeding of the workshop , 13-16 February 2002, CERN, arXiv:hep-ph/0304132v2.
- [3] In the literature another notation is also used, that is  $\phi_1$ ,  $\phi_2$ , and  $\phi_3$  for  $\beta$ ,  $\alpha$ , and  $\gamma$ , respectively.
- [4] B. Aubert *et al.* (*BABAR* Collaboration), Nucl. Instr. Meth. A **479**, 1 (2002).
- [5] S. Kurokawa *et al.* (Belle Collaboration) , Nucl. Instr. Meth. A **499**, 1 (2003).
- [6] B. Aubert *et al.* (*BABAR* Collaboration), Phys. Rev. Lett. **87**, 091801 (2001); K. Abe *et al.* (Belle Collaboration), Phys. Rev. Lett. **87**, 091802 (2001).

- [7] B. Aubert *et al.* (*BABAR* Collaboration), Phys. Rev. Lett. **98**, 031801 (2007).
- [8] K.-F. Chen *et al.* (Belle Collaboration), Phys. Rev. Lett. **98**, 031802 (2007).
- [9] H. Ishino *et al.* (Belle Collaboration), Phys. Rev. Lett. **98**, 211801 (2007); B. Aubert *et al.* (*BABAR* Collaboration), Phys. Rev. Lett. **99**, 021603 (2007).
- [10] B. Aubert *et al.* (*BABAR* Collaboration), Phys. Rev. D **79**, 072009 (2009).
- [11] M. Sigamani, Measurements of the Partial Branching Fraction for  $\bar{B} \rightarrow X_u l \bar{\nu}$  and the Determination of  $|V_{ub}|$ . Proceed. 35<sup>th</sup> Int. Conf. High Energy Phys. 2010 , PoS(ICHEP 2010) 265.
- [12] B. O. Lange, M. Neubert, and G. Paz, Phys. Rev. D **72**, 073006 (2005).
- [13] P. Gambino, P. Giordano, G. Ossola, and N. Uraltsev, JHEP **0710**, 058 (2007).
- [14] J. R. Anderson and E. Gardi, JHEP **0601**, 097 (2006).
- [15] U. Aglietti *et al.*, Eur. Phys. J. C **59**, 831 (2009).
- [16] P. Urquijo *et al.* (Belle Collaboration), Phys. Rev. Lett. **104**, 021801 (2010).
- [17] P. del Amo Sanchez *et al.* (*BABAR* Collaboration), Phys. Rev. D **83**, 032007 (2011).
- [18] N. Isgur *et al.*, Phys. Rev. D **39**, 799 (1989); D. Scora and N. Isgur, Phys. Rev. D **52**, 2783 (1995).
- [19] P. Ball and R. Zwicky, JHEP **0110**, 019 (2001); Phys. Rev. D **71**, 014015 (2005).
- [20] G. Duplancic *et al.*, JHEP **804**, 14 (2008).
- [21] E. Gulez *et al.* (HPQCD Collaboration), Phys. Rev. D **73**, 074502 (2006); erratum Phys. Rev. D **71**, 119906 (2007).
- [22] C. Amsler *et al.* (Particle Data Group), Phys. Lett. B **667**, 1 (2008).
- [23] C. G. Boyd, B. Grinstein, and R. F. Lebed, Phys. Rev. Lett. **74**, 4603 (1995); C. G. Boyd and M. J. Savage, Phys. Rev. D **56**, 303 (1997); T. Becher and R. J. Hill, Phys. Lett. B **633**, 61 (2006).
- [24] J. Bailey *et al.* (Fermilab and MILC Collaboration), Phys. Rev. D **79**, 054507 (2009).
- [25] W. -S. Hou, Phys. Rev. D **48**, 2342 (1993); A. G. Akeroyd and S. Recksiegel, J. Phys. G **29**, 2311 (2003).
- [26] B. Aubert *et al.* (*BABAR* Collaboration), Phys. Rev. D **81**, 051101(R) (2010).
- [27] P. del Amo Sanchez *et al.* (*BABAR* Collaboration), Evidence for  $B^+ \rightarrow \tau^+ \nu_\tau$  decays using hadronic B tags, arXiv: 1008.0104v1 [hep-ex].
- [28] K. Ikado *et al.* (Belle Collaboration), Phys. Rev. Lett. **97**, 251802 (2006).
- [29] K. Hara *et al.* (Belle Collaboration), Phys. Rev. D **97**, 071101 (R) (2006).

- [30] The UTfit Collaboration, <http://www.utfit.org>
- [31] The CKMfitter Collaboration, <http://ckmfitter.in2p3.fr>
- [32] O. Buchmüller and H. U. Fläcker, Phys. Rev. D **73**, 073008 (2006); C. Schwanda *et al.* (Belle Collaboration), Phys. Rev. D **78**, 032016 (2008).
- [33] B. Aubert *et al.* (BABAR Collaboration), Phys. Rev. D **79**, 012002 (2009) and references therein.
- [34] B. Aubert *et al.* (BABAR Collaboration), Phys. Rev. Lett. **104**, 011802 (2010).
- [35] N. Isgur and M. B. Wise, Phys. Lett. B **237**, 527 (1990).
- [36] I. Caprini, L. Lellouch, and M. Neubert, Nucl. Phys. B **530**, 153 (1998).
- [37] M. Okamoto *et al.*, Nucl. Phys. B, Proc. Suppl. **140**, 461 (2005).
- [38] G. M. de Divitiis *et al.*, Phys. Lett. B **655**, 45 (2007).
- [39] D. Asner *et al.* (HFAG), Averages of b-hadron, c-hadron, and  $\tau$ -lepton Properties, arXiv:1010.1589.
- [40] B. Aubert *et al.* (BABAR Collaboration), Phys. Rev. D **79**, 072009 (2009).
- [41] K. -F. Chen *et al.* (Belle Collaboration), Phys. Rev. Lett. **98**, 031802 (2007).
- [42] M. Gronau and D. London, Phys. Rev. Lett. **65**, 3381 (1990).
- [43] H. R. Quinn and A. E. Snyder, Phys. Rev. D **48**, 2139 (1993); H. R. Quinn and J. P. Silva, Phys. Rev. D **62**, 054002 (2000).
- [44] Y. Grossman and H. R. Quinn, Phys. Rev. D **58**, 017504 (1998); J. Charles, Phys. Rev. D **59**, 054007 (1999); M. Gronau *et al.*, Phys. Lett. B **514**, 315 (2001).
- [45] B. Aubert *et al.* (BABAR Collaboration), Phys. Rev. Lett. **102**, 141802 (2009).
- [46] B. Aubert *et al.* (BABAR Collaboration), Phys. Rev. Lett. **97**, 261801 (2006).
- [47] B. Aubert *et al.* (BABAR Collaboration), Phys. Rev. D **76**, 052007 (2007).
- [48] B. Aubert *et al.* (BABAR Collaboration), Phys. Rev. D **78**, 071104 (2008).
- [49] For the  $a_1(1260)$  meson we use the short notation  $a_1$ .
- [50] R. Aleksan *et al.*, Nucl. Phys. B **361**, 141 (1991).
- [51] B. Aubert *et al.* (BABAR Collaboration), Phys. Rev. Lett. **97**, 051802 (2006).
- [52] B. Aubert *et al.* (BABAR Collaboration), Phys. Rev. Lett. **98**, 181803 (2007).
- [53] M. Gronau and J. Zupan, Phys. Rev. D **73**, 057502 (2006); Phys. Rev. D **70**, 074031 (2004).
- [54] B. Aubert *et al.* (BABAR Collaboration), Phys. Rev. Lett. **100**, 051803 (2008).

- [55] K. Nakamura *et al.*(Particle Data Group) , J. Phys. G **37**, 075021 (2010).
- [56] B. Aubert *et al.* (*BABAR* Collaboration), Phys. Rev. D **81**, 052009 (2010).
- [57] C. Daum *et al.* (ACCMOR Collaboration), Nucl. Phys. B **187**, 1 (1981).
- [58] I. J. R. Aitchison, Nucl. Phys. A **189**, 417 (1972).
- [59] M. Gronau and D. Wiler, Phys. Lett. B **265**, 172 (1991); M. Gronau and D. London, Phys. Lett. B **253**, 483 (1991).
- [60] D. Atwood, I. Dunietz, and A. Soni, Phys. Rev. Lett. **78**, 3257 (1997); Phys. Rev. D **68**, 036005 (2001).
- [61] A. Giri, Y. Grossman, A. Soffer, and J. Zupan, Phys. Rev. D **68**, 054018 (2003).
- [62] P. del Amo Sanchez *et al.* (*BABAR* Collaboration), Phys. Rev. D **82**, 072004 (2010).
- [63] P. del Amo Sanchez *et al.* (*BABAR* Collaboration), Phys. Rev. D **82**, 072006 (2010).
- [64] P. del Amo Sanchez *et al.* (*BABAR* Collaboration), Phys. Rev. Lett. **105**, 121801 (2010).
- [65] B. Aubert *et al.* (*BABAR* Collaboration), Phys. Rev. D **78**, 034023 (2008); Phys. Rev. Lett. **95**, 121802 (2005).
- [66] A. Poluektov *et al.* (Belle Collaboration), Phys. Rev. D **81**, 112002 (2010); Phys. Rev. D **73**, 112009 (2006).
- [67] <http://lhcb.web.cern.ch/lhcb/>
- [68] <http://superb.kek.jp/>
- [69] <http://web.infn.it/superb/>